2016

An implementation of the relativistic hydrodynamic equations in conservative form using Dogpack

Milo Thomas Taylor
Iowa State University

An implementation of the relativistic hydrodynamic equations in conservative form using Dogpack

by

Milo Taylor

A thesis submitted to the graduate faculty
in partial fulfillment of the requirements for the degree of
MASTER OF SCIENCE

Major: Applied Mathematics

Program of Study Committee:
James Rossmanith, Major Professor
Paul Sacks
Michael Young

Iowa State University
Ames, Iowa
2016

DEDICATION

Dedicated to my family and friends. This thesis is written in memory of my tutu, Myrna, who always pushed her grandchildren to not be lazy and to be grateful.

TABLE OF CONTENTS

LIST OF FIGURES

ACKNOWLEDGEMENTS

I would like to thank my thesis advisor and research group leader, Dr. James Rossmanith of Mathematics Department of Iowa State University for his support and patience in my research endeavors. Without his guidance, much of the material in this thesis may very well have been a mystery to me. His expertise in the mathematics and familiarity in the physics proved invaluable.

I would also like to acknowledge my other Program of Study Committee members, Drs. Paul Sacks and Michael Young for agreeing to evaluate my understanding of the material. They have also taught me a great deal in different areas of mathematics as well as some valuable life lessons and opportunities that I would not have had access to on my own.

Lastly, I would like to express my deep gratitude to my family and my beloved for sympathizing with my efforts to produce my own research in this field that I hope to one day become an expert in. They have also lent their support even though they are either working on their own theses or are moving to the next step in their life and careers.

ABSTRACT

Let $g_{\mu\nu}$ be the metric associated with a stationary spacetime. In the $3+1$ splitting of spacetime, this allows us to cast the relativistic hydrodynamic equations as a balance law of the form $q_{,t} + \nabla \cdot \mathbf{F}(q) = \mathbf{S}$, which is a system of hyperbolic partial differential equations. These hyperbolic equations admit shocks and rarefactions in their weak solutions. Because of this, we employ a Runge-Kutta Discontinuous Galerkin method in both Minkowski and Schwarzschild spacetimes through the use of the Discontinuous Galerkin Package. In this thesis, we give a quick background on topics in general relativity necessary to implement the method, as well as details on the DG method itself. We present tests of the method in the form of shock tube tests and smooth flow into a black hole to show its versatility.

CHAPTER 1. INTRODUCTION AND SCOPE

1.1 Purpose of the Thesis

This thesis is meant to test the viability and to show the advantages of solving the relativistic hydrodynamics equations using discontinuous Galerkin methods. While these methods are employed in recent works [14], their implementation is still in its infancy. This work is intended neither to be comprehensive review nor as a mathematical monograph. Rather, it serves as the author's current understanding of the subject material, and his ability to add meaningful research to the field.

1.2 Scope of the Thesis

The contents of this thesis, starting with Chapter 2, are organized as follows

- **Chapter 2**: A Brief Review of the Mathematics of Relativity
  - + We introduce the notion of tensors in spacetime, including the metric and the quantities which describe it. We also provide details in the 3+1 splitting of spacetime, and how it pertains to this thesis.
- **Chapter 3**: Relativistic Hydrodynamics: Special and General
  - + In this chapter, we provide the hydrodynamics equations in multiple forms. One such is the conservative form of the equations, which is the main focus of Chapter 3 and those following.
- **Chapter 4**: Numerical Methods

  + We give a description of the numerical method employed, a discontinuous Galerkin method, as well as means to ensure high order accuracy. Topics such as shocks and limiters are also detailed.

- **Chapter 5**: Tests and Results

  + The shock tube test for special relativity and the simulation of dust accretion onto a black hole are described. Results on these two test cases are also provided.

- **Chapter 6**: Future Work

  + Several avenues to pursue research are briefly described in this chapter. This thesis is meant as groundwork for the author to contribute to the aspects laid out in the final chapter.

The layout of the thesis is meant to ease the reader into the thesis topic. We begin with a few key details of Einstein's theory of relativity that can be studied more in works like [18] or [3]. This is the chapter where we build the tools necessary to describe phenomena at extremely high speeds or even in curved spacetimes. We then move to describe the evolution of a perfect fluid both in general and in the relativistic setting. These are heavily detailed in [8] and [14]. The decription of the numerical methods follow suit, and are explained in-depth in works like [12]. Finally, we show results of a select number of test cases in special and general relativity.

CHAPTER 2. A BRIEF REVIEW OF THE MATHEMATICS OF RELATIVITY

We begin with a description of spacetime in the language of Albert Einstein's theory of relativity. In this chapter, we establish the notion of spacetime as well as develop mathematical objects within it. This chapter covers only the basics of a few topics in relativity. Refer to [18, 3, 14] for more details.

2.1 Minkowski Spacetime

A spacetime $\mathcal{M}$ may be thought of a collection of points called events. More specifically, we have the following definition.

Definition 2.1 *An* ***event*** $\mathcal{P}$ *is a point in a spacetime* $\mathcal{M}$ *that describes a location and time according to an observer* $\mathcal{O}$*.*

2.1.1 Coordinates

Typically, any coordinates given or referenced to in this thesis are with respect to an inertial reference frame. In simple terms, an inertial reference frame is a non-accelerating, non-rotating piece of spacetime.

We overlay the spacetime with a coordinate system $\{x^\mu\}$ or $\{x^{\mu'}\}$ where $\mu, \mu' = 0, 1, 2, 3$. Examples of this are Cartesian coordinates (t, x, y, z) and spherical polar coordinates (t, r, θ, ϕ). In either system, we are describing the same spacetime. This leads to the notion of a *coordinate transformation* $\{x^\mu\} \to \{x^{\mu'}\}$ which takes one coordinate system and describes all points in the spacetime in the second coordinate system.

Definition 2.2 *Consider two events $\mathcal{P}_1$ and $\mathcal{P}_2$ in the spacetime with Cartesian coordinates (t_1, x_1, y_1, z_1) and (t_2, x_2, y_2, z_2), respectively. The* ***Minkowski spacetime interval*** *is given by*

$$(\Delta s)^2 = -(\Delta t)^2 + (\Delta x)^2 + (\Delta y)^2 + (\Delta z)^2 \tag{2.1}$$

where $\Delta x^\mu := x_2^\mu - x_1^\mu$ [3]. Equation (1.1) is often called the line element. This quadratic form is akin to the familiar Pythagorean theorem. Minkowski spacetime is the spacetime of special relativity.

Let $\mathcal{O}$ be a reference frame and $\overline{\mathcal{O}}$ be another moving at a speed v relative to $\mathcal{O}$. Then due to the invariance of the speed of light, we find that

$$(\Delta s)^2 = (\Delta \bar{s})^2. \tag{2.2}$$

So the spacetime interval is an invariant under the above conditions.

2.1.2 Four-Vectors and One-Forms

In order to build notions of displacement, velocity, and other fundamental objects, we must first formalize the idea of a vector in spacetime. We must also introduce the idea of a one-form whose connection to vectors are described in the upcoming sections. In the following definitions, we use the standard notation for a *Lorentz transformation*, e.g.

$$\Lambda^{\bar{\alpha}}{}_{\beta} := \frac{\partial x^{\bar{\alpha}}}{\partial x^\beta} \tag{2.3}$$

which may be thought of a matrix that allows vectors expressed in one set of coordinates to be expressed in another.

Definition 2.3 *A* ***four-vector*** **V** *is a collection of four numbers $\{V^\alpha\}$ which transform from frame $\mathcal{O}$ to another frame $\bar{\mathcal{O}}$ by*

$$V^{\bar{\alpha}} = \Lambda^{\bar{\alpha}}{}_{\beta} V^\beta. \tag{2.4}$$

Definition 2.4 *A **one-form** $\tilde{p}$ is a collection of four numbers $\{p_\alpha\}$ which transform from frame $\mathcal{O}$ to another frame $\bar{\mathcal{O}}$ by*

$$p_{\bar{\beta}} = \Lambda^{\alpha}{}_{\bar{\beta}} p_\alpha. \tag{2.5}$$

In this thesis, we make extensive use of *Einstein summation notation* when describing objects in special and general relativity, such as those decribed in this section. In this convention, repeated indices indicate an implied sum so that, for instance

$$\begin{aligned} V^\alpha p_\alpha &= U^0 p_0 + U^1 p_1 + U^2 p_2 + U^3 p_3, \\ V^i p_i &= V^1 p_1 + V^2 p_2 + V^3 p_3. \end{aligned} \tag{2.6}$$

Note that Greek indices $\alpha, \beta, \gamma, \ldots$ run through $\{0, 1, 2, 3\}$ while Roman indices $i, j, k, \ldots$ run through $\{1, 2, 3\}$ as per standard convention.

At the risk of foreshadowing the connection between four-vectors and one-forms, we may refer to either as simply "vectors".

2.1.3 Tensors

Now that we have a firm grasp on the notion of a four-vector, we consider functions mapping to and from sets of them. One of the simplest examples takes two vectors and produces a scalar. For two vectors $\mathbf{a}$ and $\mathbf{b}$, a *tensor* $\mathbf{T}$ may be defined as

$$\mathbf{T}(\mathbf{a}, \mathbf{b}) = c,$$

for some scalar c. Note that this is not *the* definition of a tensor. Rather, it is an example of one. To delve further, we take a moment to recall the component form of a vector $\mathbf{a}$. The vector can be described in contravariant form a^μ or covariant form a_μ given a specific coordinate system.

Likewise, we may express a tensor in terms of components. For example, the tensor described above may be thought of as a matrix of 16 components. If a^μ and b^ν are given, we express the tensor in the *covariant form* $T_{\mu\nu}$. Alternatively, we would use the *contravariant*

form $T^{\mu\nu}$ given a_μ and b_ν, or the mixed tensor $T^\mu{}_\nu$ given a_μ and b^ν. The three represent the *same* tensor in some sense. Throughout this thesis, references to a given tensor will be to its components unless otherwise stated.

Tensors are not limited to only two indices. Generally speaking, a tensor is a generalization of a vector or covector.

Definition 2.5 *A* ***tensor*** **T** *of type* (p, q)*, where* p, q *are nonnegative integers, is a multilinear map from a collection of one-forms and vectors to* $\mathbb{R}$ *[3].*

In light of this definition, we classify a scalar as a $(0, 0)$-tensor, a vector as a $(1, 0)$-tensor, and a one-form as a $(0, 1)$-tensor. Moreover, while the definition suggests tensors map to scalars, we may still apply a tensor to a single vector to yield a vector; this is why the word "collection" is used. As an example, we may have

$$T^\mu{}_\nu : a^\nu \mapsto T^\mu{}_\nu a^\nu.$$

A (p, q)-tensor may take up to p one-forms and up to q vectors to produce a scalar or tensor. For example, applying a (p, q)-tensor to $p - 1$ one-forms and $q - 2$ vectors produces a $(1, 2)$-tensor. The $(1, 1)$-tensor above takes no one-forms and a single vector to produce a vector $v^\mu := T^\mu{}_\nu a^\nu$, which is a $(1, 0)$-tensor.

A defining property of a tensor is how it transforms from one coordinate system $\{x^\mu\}$ to another $\{x^{\mu'}\}$. We have the contravariant *transformation laws*

$$\begin{aligned} T^{\bar{\mu}\bar{\nu}} &= \frac{\partial x^{\bar{\mu}}}{\partial x^\mu}\frac{\partial x^{\bar{\nu}}}{\partial x^\nu}T^{\mu\nu}, \\ &= \Lambda^{\bar{\mu}}{}_\mu \Lambda^{\bar{\nu}}{}_\nu T^{\mu\nu}. \end{aligned} \tag{2.7}$$

There are analogous laws for tensors of different rank, but the idea is the same: a Lorentz transformation for each index. We will see a linear transformation in the next section that *does not* follow this kind of a transformation law, thus not qualifying as a tensor.

2.1.4 The Metric

In describing Einstein summation notation above, (2.6) leads to a useful definition.

Definition 2.6 *The* ***scalar product*** *between two four-vectors* $\mathbf{U}$ *and* $\mathbf{V}$ *is denoted by* $\mathbf{U} \cdot \mathbf{V}$ *and is given by*

$$\mathbf{U} \cdot \mathbf{V} := \mathbf{g}(\mathbf{U}, \mathbf{V}) = g_{\mu\nu} U^\mu V^\nu \tag{2.8}$$

where $\mathbf{g}$ *is the* ***metric****.*

The metric is essential; indeed it is the single most important tensor in relativity. In Minkowski spacetime, the metric and its components are denoted by $\eta_{\mu\nu}$ instead of $g_{\mu\nu}$ due to its importance and prevalance. The components of this specific metric in Cartesian coordinates (t, x, y, z) are

$$\eta_{\mu\nu} = \begin{pmatrix} -1 & 0 & 0 & 0 \\ 0 & 1 & 0 & 0 \\ 0 & 0 & 1 & 0 \\ 0 & 0 & 0 & 1 \end{pmatrix}.$$

The matrices representing the metric $\eta_{\mu\nu}$ and its counterpart $\eta^{\mu\nu}$ are the same. In general, this is not the case. However, the metric is always symmetric and is such that

$$g^{\alpha\gamma} g_{\gamma\beta} = g^\alpha{}_\beta = \delta^\alpha{}_\beta. \tag{2.9}$$

That is, the covariant and contravariant forms of the metric are inverses of one another. Indeed, this is an especially important property. The metric and its inverse are used in order to "raise" or "lower" indices [18]. In particular, they provide a connection between a vector and its one-form counterpart. For a vector $\mathbf{V}$ we have

$$V^\alpha = g^{\alpha\beta} V_\beta, \tag{2.10}$$

$$V_\alpha = g_{\alpha\beta} V^\beta. \tag{2.11}$$

There is a very important relationship between the metric and the line element:

$$ds^2 = g_{\alpha\beta}\, dx^\alpha\, dx^\beta, \tag{2.12}$$

which is why we dub **g** the metric: it is at the center of this "distance formula". For example, the line element associated with *Minkowski spacetime* in **Def 2.2** is given by

$$\begin{aligned} ds^2 &= \eta_{\alpha\beta}\, dx^\alpha\, dx^\beta \\ &= -dt^2 + dx^2 + dy^2 + dz^2, \end{aligned} \tag{2.13}$$

in Cartesian coordinates.

We are also concerned with derivatives of the metric. Specifically, the following definition will prove useful in defining divergence in spacetime, discussed in the upcoming section.

Definition 2.7 *The* ***Christoffel symbols*** Γ *are linear transformations whose components are*

$$\Gamma^\alpha_{\beta\gamma} = \frac{1}{2} g^{\alpha\delta} \left(\frac{\partial}{\partial x^\gamma} g_{\delta\gamma} + \frac{\partial}{\partial x^\beta} g_{\delta\gamma} - \frac{\partial}{\partial x^\delta} g_{\beta\gamma} \right). \tag{2.14}$$

While the Christoffel symbols are in fact linear transformations, they are not tensors. The Christoffel symbols do not transform like rank 3 tensors.

Another reason why we denote the metric of Minkowski spacetime (for special relativity) is that, in order to properly deal with curved manifolds, we have the idea of a *local Lorentz frame* at an event $\mathcal{P}$ ([18], p 146):

$$\begin{aligned} g_{\alpha\beta}(\mathcal{P}) &= \eta_{\alpha\beta} \quad \text{for all } \alpha, \beta \\ \frac{\partial}{\partial x^\gamma} g_{\alpha\beta}(\mathcal{P}) &= 0 \quad \text{for all } \alpha, \beta, \gamma \\ \frac{\partial^2}{\partial x^\gamma \partial x^\mu} g_{\alpha\beta}(\mathcal{P}) &\neq 0 \quad \text{in general.} \end{aligned} \tag{2.15}$$

.

Although we do not explicitly use the notion of local Lorentz frames in this thesis, they are an underlying idea that connects many equations from flat spacetime to curved. These frames also allow us to perform differentiation of tensors even though a vector at an event $\mathcal{P}_1$ lives in a separate so-called tangent space than a vector at an event $\mathcal{P}_2$.

2.2 Divergence in Spacetime

In order to properly describe the governing equations of relativistic hydrodynamics, we briefly describe what the appropriate notion of a divergence is in spacetime, which is non-Euclidean. For ease of notation, we adopt the convention of expressing the derivative of a tensor with respect to some coordinate with a comma and index. That is, for example, for a tensor $\mathbf{T}$ we write

$$T^{\alpha\beta}{}_{,\gamma} := \frac{\partial}{\partial x^\gamma} T^{\alpha\beta} \quad \text{and} \quad T_{\alpha\beta,\gamma} := \frac{\partial}{\partial x^\gamma} T_{\alpha\beta}. \tag{2.16}$$

With this notation, the traditional divergence of a vector field, say V^α, is a scalar given by

$$\nabla \cdot \mathbf{V} = V^\alpha{}_{,\alpha} = \frac{\partial V^0}{\partial x^0} + \frac{\partial V^1}{\partial x^1} + \frac{\partial V^2}{\partial x^2} + \frac{\partial V^3}{\partial x^3}.$$

Definition 2.8 *The **covariant derivative of a four-vector** $\mathbf{V}$ is a $(1,1)$-tensor whose components are denoted as $V^\alpha{}_{;\beta}$ and are given by*

$$(\nabla_\beta \mathbf{V})^\alpha := V^\alpha_{;\beta} := V^\alpha_{,\beta} + \Gamma^\alpha{}_{\mu\beta} V^\mu. \tag{2.17}$$

.

There is a similar definition of the covariant derivative for a one-form, but it is virtually identical and inconsequential in this work. However, we do need the following definition:

Definition 2.9 *The **covariant derivative of a** $(2,0)$ **tensor** $T^{\mu\nu}$ is a $(2,1)$ tensor whose components are denoted as $T^{\mu\nu}{}_{;\lambda}$ and are given by*

$$T^{\mu\nu}{}_{;\lambda} = T^{\mu\nu}_{,\lambda} + T^{\alpha\nu}\Gamma^\mu_{\alpha\lambda} + T^{\mu\alpha}\Gamma^\nu_{\alpha\lambda}. \tag{2.18}$$

The definitions for other kinds of tensors are similarly defined [18, 3]. As a general rule, upstairs components correspond to adding Christoffel symbols while downstairs components correspond to subtracting them. The one-form analogue to (2.17) switches the sign in front of the Christoffel symbols, for example. Due to the usage of ∇ in the upcoming chapters for the usual divergence in $\mathbb{R}^n$, we use the component form of the covariant derivative henceforth.

2.3 Spacetime of a Stellar Object

What does spacetime "look like" near the Sun or any other spherical celestial body? Part of this thesis is concerned with hydrodynamic flow near a black hole. We must be able to model a fluid accreting into a black hole, or at least a star. In $G = c = 1$ units, the metric *outside* of a spherical mass M which is nonrotating and uncharged can be modeled via the following line element

$$ds^2 = -\left(1 - \frac{2M}{r}\right) dt^2 + \left(1 - \frac{2M}{r}\right)^{-1} dr^2 + r^2\, d\Omega^2, \tag{2.19}$$

with $d\Omega^2 := d\theta^2 + \sin^2\theta\, d\phi^2$ [19]. The corresponding metric $g_{\mu\nu}$ is widely known as the *Schwarzschild metric*, where $r_s = 2M$ is known as the Schwarzschild radius. Since the mass of a black hole is typically far greater than any surrounding object, the metric above gives a good approximation. It is important to note that the Schwarzschild metric can only describe nonrotating objects, although physical black holes do have angular momentum.

We consider a few of the properties of this spacetime:

Stationary. The metric does not depend on time. As an aside, it turns out that this is not due to the fact that the star or black hole is not rotating.

Spherically symmetric. This is to be expected, given that the metric describes the spacetime surrounding a spherical body such as a black hole.

Singularities. Upon further inspection, two singularities are apparent:

1. As $r \to 0$, the dt^2 term of (2.19) blows up.
2. As $r \to 2M$, the Schwarzschild radius, the radial term of (2.19) blows up. However, unlike the above, this is simply a coordinate singularity. In the next section, we investigate.

2.3.1 Eddington-Finkelstein Coordinates

In order to remedy the apparent singularity at $r = 2M$ in the line element (2.19) we define a new coordinate, the so-called tortoise coordinate [3, 18],

$$r^* = r + 2M \ln \left| \frac{r}{2M} - 1 \right|. \tag{2.20}$$

The (ingoing) coordinates give the line element

$$ds^2 = -\left(1 - \frac{2M}{r}\right) dt'^2 + \frac{4M}{r}\, dt'\, dr + \left(1 + \frac{2M}{r}\right) dr^2 + r^2\, d\Omega^2, \tag{2.21}$$

where $t' = t + (r^* - r)$. Although the metric still involves the coordinate radius r, the coordinate singularity as $r \to 2M$ has been resolved. The fact that we have a coordinate system in which this singularity disappears shows that it was nonphysical from the beginning. On the other hand, the singularity $r \to 0$ is still present, but in numerical simulations we often delete a region containing it.

2.3.2 A 3 + 1 Decomposition of Spacetime

Although we treat space and time on equal footing in relativity, we wish to specifically single out time for computational reasons. This would allow us to evolve the to-be discussed hydrodynamic equations in time using explicit methods.

We may foliate spacetime into a family of constant-time hypersurfaces $\Sigma(t)$ [1, 14]. On a single given hypersurface of such, Σ_t, we can identify a timelike four-vector $\mathbf{n}$ which is normal to Σ_t. The components of this normal vector are written as

$$n_\mu = (-\alpha, 0, 0, 0), \qquad n^\mu = \frac{1}{\alpha}(1, -\beta^i). \tag{2.22}$$

The lapse function α and shift vector β define the foliated spacetime. They will be the quantities we actually use to define the foliation. The line element in this $3 + 1$ decomposition of spacetime would be

$$ds^2 = -(\alpha^2 - \beta_i \beta^i)\, dt^2 + 2\beta_i\, dx^i\, dt + \gamma_{ij}\, dx^i\, dx^j, \tag{2.23}$$

where we define the *spatial metric*

$$\gamma_{\mu\nu} = g_{\mu\nu} + n_\mu n_\nu, \qquad \gamma^{\mu\nu} = g^{\mu\nu} + n^\mu n^\nu \tag{2.24}$$

which has the properties: $\gamma^{0\mu} = 0$ (hence spatial), $\gamma_{ij} = g_{ij}$, and $\gamma^{ik}\gamma_{kj} = \delta^i_j$. We may thus use γ in order to raise and lower indices of four-vectors defined entirely on Σ_t. For instance, the *spatial four-velocity* $\mathbf{v}$, which is defined as

$$v^\mu = \left(0, \frac{1}{\alpha}\left(\frac{u^i}{u^t} + \beta^i\right)\right)^T, \tag{2.25}$$

$$v_\mu = \left(\beta_j v^j, \frac{u_i}{W}\right), \tag{2.26}$$

is such that v_μ is not a fully spatial one-form so we cannot raise v_i using the spatial metric γ^{ij}–we must use the full metric, $g^{\mu\nu}$. On the other hand, the shift vector β is spatial so that

$$\beta^i = \gamma^{ij}\beta_j \quad \text{and} \quad \beta_i = \gamma_{ij}\beta^j. \tag{2.27}$$

The metric $\mathbf{g}$ can then be written in covariant and contravariant form succinctly

$$g_{\mu\nu} = \begin{pmatrix} -\alpha^2 + \beta_i\beta^i & \beta_i \\ \beta_i & \gamma_{ij} \end{pmatrix}, \qquad g^{\mu\nu} = \begin{pmatrix} -1/\alpha^2 & \beta^j/\alpha^2 \\ \beta^i/\alpha^2 & \gamma^{ij} - \beta^i\beta^j/\alpha^2 \end{pmatrix}, \tag{2.28}$$

which leads to the useful identity

$$\sqrt{-g} = \alpha\sqrt{\gamma}, \tag{2.29}$$

where $g :=\det(g_{\mu\nu}) \leq 0$ and $\gamma :=\det(\gamma_{\mu\nu}) \geq 0$ [14]. As can be seen in (2.9), the essential information from the foliation are, in fact, α and β with γ_{ij} describing the individual slices. In general, there is freedom in choosing these values, but some choices are better than others. For instance, choosing $\alpha = 1$ can result in serious issues in simulations "due to the tendency of timelike geodesics without vorticity... to focus and eventually cross "[5]. That is, the foliation would only allow us to evolve the system to a finite value of time T, as opposed to some arbitrary time t.

For the ingoing Eddington-Finkelstein metric, we have

$$\begin{aligned} \alpha &= \left(1+\frac{2M}{r}\right)^{-1/2}, \\ \beta_i &= \left(\frac{2M}{r},0,0\right), \\ \beta^i &= \left(\frac{2M}{r}\left(1+\frac{2M}{r}\right)^{-1},0,0\right), \\ \gamma_{ij} &= \mathrm{diag}\left(1+\frac{2M}{r},r^2,r^2\sin^2\theta\right). \end{aligned} \tag{2.30}$$

The *extrinsic curvature* $K_{\mu\nu}$ is a tensor which provides information on how Σ_t connects to the full spacetime. The extrinsic curvature, as the name would suggest, is a measure of how Σ_t is curved within the spacetime. It is defined to be

$$K_{\mu\nu} := -\gamma^{\lambda}{}_{\mu}\nabla_{\lambda}n_{\nu}. \tag{2.31}$$

It should be noted that K_{ij} can be written in terms of the Lie derivative of γ_{ij}, but that is beyond the scope of this work. As we shall see at the end of this chapter, the extrinsic curvature reduces to spatial derivatives of the spatial metric within the context of the hydrodynamical equations at hand. For more in depth information, see for example [14, 5].

It should be noted that this splitting of spacetime is especially useful in simulations involving *dynamic* spacetimes. One such prototypical example is a TOV star. These kinds of simulations require the hydrodynamic equations to describe the motion of fluids and the Einstein equations to describe the evolving spacetime itself.

CHAPTER 3. RELATIVISTIC HYDRODYNAMICS: SPECIAL AND GENERAL

The equations that describe a fluid undergoing relativistic speeds or flowing in a region with strong gravitational effects are known as the *relativistic hydrodynamic equations*, *Einstein-Euler equations*, or the *relativistic Euler equations*. In this work we largely refer to them by the first since the Einstein-Euler equations may be regarded as the hydrodynamic equations coupled with the Einstein equations.

3.1 Equations for Conservation Laws

We are now suitably equipped to state and analyze the conservation laws of a relativistic fluid. These laws are five and read

$$(\rho u^{\mu})_{;\mu} = 0, \tag{3.1}$$

$$T^{\mu\nu}{}_{;\nu} = 0, \tag{3.2}$$

for $\mu, \nu = 0, 1, 2, 3$ and where $_{;\nu}$ denotes the covariant derivative with respect to the coordinate x^{ν}. Note that (3.1) is a scalar equation while (3.2) is a vector equation of four components. The quantity ρ is the rest mass density of the fluid, u^{μ} is the four-velocity, and $T^{\mu\nu}$ is the stress-energy tensor. All of these are, in general, coordinate dependent (e.g. $u^{\mu} = u^{\mu}(t, x^1, x^2, x^3)$). In other words two different elements of the fluid may have two different densities or even four-velocities.

The equations (3.1) − (3.2) are in covariant form, so are true in *any* coordinate system. Moreover, the equations are valid in both special and general relativity. As such, these are

the relativistic hydrodynamic equations. In Minkowski spacetime, the equations are simpler since the covariant derivative coincides with the divergence in Cartesian coordinates in that flat spacetime.

Since we are only concerned with perfect fluids, the stress-energy tensor is shearless and takes the form

$$T^{\mu\nu} = \rho h u^\mu u^\nu + p g^{\mu\nu}, \tag{3.3}$$

where p is the fluid pressure and h is the specific enthalpy $h = (e+p)/\rho$, and e is the energy density [14, 3]. In the special relativistic case we have $g^{\mu\nu} = \eta^{\mu\nu} = \text{diag}(-1, 1, 1, 1)$. To reflect the fact that this tensor is stress-free, we refer to it as the *energy-momentum* tensor. We can interpret the components of this tensor as

$$T^{\mu\nu} = \left(\text{flux of } \mu\text{-momentum across a surface of constant } x^\nu \right), \tag{3.4}$$

for a perfect fluid [18]. By 0-momentum we mean energy flux.

3.2 Special Relativistic Hydrodynamics Equations

For a perfect fluid in Minkowski spacetime, the special relativistic hydrodynamic (RHD) equations read

$$\partial_\mu(\rho u^\mu) = 0, \tag{3.5}$$

$$\partial_\mu(w u^\mu u^\nu + p\eta^{\mu\nu}) = 0, \tag{3.6}$$

where we define the relativistic enthalpy $w = e + p = \rho h$. In this work, the equation of state which closes the system (3.5) − (3.6) is simple and given by

$$p = (\Gamma - 1)(e - \rho), \tag{3.7}$$

with the adiabatic index $\Gamma = 5/3$ for mildly relativistic speeds and $\Gamma = 4/3$ for the ultra-relativistic scenario codified by $e \gg \rho$ [4]. We will make more use of the three-velocity, so we

make explicit that the four-velocity is defined as $u^\mu = (W, Wv^j)$, where $W = (1 - v^j v_j)^{-1/2}$ is the Lorentz factor.

3.3 On the Form of the Relativistic Hydrodynamics Equations

In order to describe a perfect fluid, we need to know at least the density, velocity, and pressure. We introduce the *primitive variables*

$$\mathbf{V} = (\rho, v_j, p) \in \mathbb{R}^5, \tag{3.8}$$

which are specifically those in that order. Note that we may use the specific energy ε rather than p since the two are linked by an equation of state. With the primitive variables $\mathbf{V}$, the hydrodynamic equations (3.1) – (3.2) turn out not to be in *conservative form*, which we will solidify below.

3.3.1 Conservative Formulation

In the literature, it can be shown that the equations of relativistic hydrodynamics can be written in *quasilinear form*

$$\partial_t \mathbf{U} + \mathbf{A} \cdot \nabla \mathbf{U} + \mathbf{B} = 0, \tag{3.9}$$

where $\mathbf{U} \in \mathbb{R}^N$ is the state vector and $\mathbf{A} \in \mathbb{R}^{N \times N}$ is diagonalizable with real eigenvalues and a set of linearly independent eigenvectors. With such a matrix $\mathbf{A}$ the system is said to be *hyperbolic* [14]. The hyperbolic nature of the equations is key in our numerical treatment and the employment of DoGPack.

If we happen to have that $\mathbf{A} = \partial \mathbf{F} / \partial \mathbf{U}$ for some *flux vector* $\mathbf{F}(\mathbf{U})$, then the homogeneous ($\mathbf{B} = 0$) form becomes a *conservation law*

$$\partial_t \mathbf{U} + \nabla \cdot \mathbf{F}(\mathbf{U}) = 0, \tag{3.10}$$

but in general we have a *balance law*

$$\partial_t \mathbf{U} + \nabla \cdot \mathbf{F}(\mathbf{U}) = \mathbf{S}, \tag{3.11}$$

where $\mathbf{S}$ is known as the *source term*. In either case, we will refer to either as *conservative form* and the state vector $\mathbf{U}$ as the *conserved variables*.

In the *Valencia formulation* [14] of the Eulerian GRHD equations, we have the conserved variables

$$D = \rho W, \tag{3.12}$$

$$S_j = \rho h W^2 v_j, \tag{3.13}$$

$$E = \rho h W^2 - p, \tag{3.14}$$

$$\tau = E - D. \tag{3.15}$$

Here, the Lorentz factor is given by $W = \alpha u^t = \left(1 - v_i v^i\right)^{-1/2}$.

Note that E and τ both represent conserved energy, so in the formulation we use only one of the two. The *state vector* is thus

$$\mathbf{U}(\mathbf{V}) = (D, S_j, \tau) \in \mathbb{R}^5. \tag{3.16}$$

The components of the projection of the energy-momentum tensor $\mathbf{T}$ onto Σ_t, denoted by $S^{\mu\nu}$, are given by

$$S^{\mu\nu} = \rho h W^2 v^\mu v^\nu + p\gamma^{\mu\nu}, \tag{3.17}$$

through little effort ([14], p 365). It is important to keep in mind the differences between the momentum S^μ, the projection $S^{\mu\nu}$, and the source $\mathbf{S}$.

In Minkowski spacetime, the equations (3.5) and (3.6) can be cast in the form (3.11) using the conserved variables $\mathbf{U}$ in (3.16) with flux

$$\mathbf{F}^i(\mathbf{U}) = (\rho W v^i, \rho h W^2 v^i v^j + p\delta^{ij}, \rho h W^2 v^i - D v^i) \in \mathbb{R}^5. \tag{3.18}$$

The hydrodynamic equations in Minkowski spacetime thus form a conservation law with $\mathbf{S} = 0$ which is highly coupled due to the presence of the Lorentz factor W. If we compare this conservation law with its Newtonian (non-relativistic) counterpart we see that the inclusion of W is the key difference [4, 14]. The non-relativistic Euler equation can be found in many texts on finit volume methods including [8].

In the update of the numerical solution, only the conserved variables are updated. Immediately, we notice an issue: the flux vector is in terms of both the primitive and conserved variables. That is, we need both to compute the flux. In the conservative formulation this is unavoidable in the sense that we cannot write the flux in terms of the conserved variables only. As such, we must invert the equations $(3.12) - (3.15)$ to obtain the primitive variables.

As pointed out by [14, 4], there is no closed form solution for this inversion due to the coupling caused by the Lorentz factor W. As a result, we must use a root-finding algorithm to find the correct W. The primitive variables could then be found using the definitions of the conserved variables. We lay out this method near the end of the next chapter.

3.3.2 The General Relativistic Euler Equations

Now that we have established a conservative formulation for the requisite variables, we now move on to the hydrodynamic equations at the center of this thesis. The relativistic hydrodynamic equations can be written as

$$\partial_t(\sqrt{\gamma}\mathbf{U}) + \partial_i(\sqrt{\gamma}\mathbf{F}^i) = \mathbf{S}, \tag{3.19}$$

with the conserved variables $\mathbf{U}$ being given by (3.16). Note that this is of the form (3.11). In general, the determinant γ depends on coordinates, so we cannot divide it out. The flux

vector is given by

$$\mathbf{F}^i = \begin{pmatrix} (\alpha v^i - \beta^i)D \\ \alpha S^i{}_j - \beta^i S_j \\ \alpha(S^i - Dv^i) - \beta^i \tau \end{pmatrix}. \tag{3.20}$$

As suggested by the notation, there are three flux vectors $\mathbf{F}^1$, $\mathbf{F}^2$, and $\mathbf{F}^3$–one for each spatial direction.

The source term $\mathbf{S}$ is nonzero in general and takes the form

$$\mathbf{S} = \sqrt{\gamma} \begin{pmatrix} 0 \\ \frac{1}{2}\alpha S^{ik}\partial_j \gamma_{ik} + S_i \partial_j \beta^i - E\partial_j \alpha \\ \alpha S^{ij} K_{ij} - S^j \partial_j \alpha \end{pmatrix}. \tag{3.21}$$

As written, the source term is valid even for time-dependent metrics. However, as we have seen, the Schwarzschild spacetime in any valid coordinate system is stationary; it does not depend on time. Given this, it can be shown that

$$\alpha S^{ik} K_{ik} = \frac{1}{2} S^{ik} \beta^j \partial_j \gamma_{ik} + S^j{}_i \partial_j \beta^i, \tag{3.22}$$

so that we need not worry about the extrinsic curvature ([14], p 367). It should be noted that rather than using the extrinsic curvature, we could have expressed (3.21) in terms of Christoffel symbols, which is how the relativistic hydrodynamic equations were first presented by Banyuls *et al* [1]. Both ways are mathematically equivalent, and since the spacetime is stationary these amount to only the spatial derivatives of the spatial metric.

In the next chapter, we shall delve deeper into how to implement the equations (3.19) in order to simulate phenomena ranging from astrophysical jets to matter accreting into a black hole.

CHAPTER 4. NUMERICAL METHODS

Now that we have a solid understanding of some key concepts in general relativity, we move on to a numerical treatment of the Einstein-Euler equations. In this chapter, we discuss the numerical method employed in the DoGPack code. That is, we present the framework and advantages of discontinuous Galerkin methods.

As a disclaimer, we denote a generic set of variables by q in the bulk of this chapter. Of course, we may choose to think of $q \to \sqrt{\gamma}\mathbf{U}$ to obtain the relativistic hydrodynamic equations more explicitly.

4.1 The Basics

To describe how well our DG method approximates the actual solution, we must conduct convergence studies on our simulations. We begin with defining what we might measure as the error. The *local error* is simply the difference between the numerical solution U_j^n and the exact solution sampled on the mesh $u^h(t^n, x_j)$ where h is the grid spacing in the one-dimensional case. That is, at time $t = t^N$, the local error is

$$E_j^h := U_j^N - u^h(t^N, x_j).$$

We can use the max norm in order to gain a sense of a *global error*

$$E^h := \|E^h\|_\infty = \max_j(E_j^h).$$

Convergence in this norm ensures pointwise convergence by its very definition. If we find the numerical solution using different grid spacings h and k with $k < h$, then the *global order*

of accuracy given by

$$p := \frac{\log(E^h/E^k)}{\log(h/k)}. \tag{4.1}$$

In other words, we seek the slope p of the line when plotting $\log E$ against $\log h$ [14, 8].

To introduce the next idea, we must define the true and numerical domains of dependence. The *true domain of dependence* of a point (x_j, t^{n+1}) is the set of points at time $t = t^n$ that the solution depends on. This domain can be determined using the characteristics that arrive at (x_j, t^{n+1}). On the other hand, the *numerical domain of dependence* is simply the set of points at time $t = t^n$ that are actually used in the calculation [14, 9]. While the numerical domain is under the control of whoever seeks to solve the PDE numerically, the true domain is inherent in the problem itself.

The *CFL condition* states that "a numerical method can be convergent only if its numerical domain of dependence contains the true domain of dependence of the PDE, at least in the limit as Δt and Δx go to zero" [LeVeque 52]. This is a necessary condition for the stability and convergence of a numerical method.

In practice, the CFL condition amounts imposing the relationship

$$\Delta t \leq c_{CFL} \min\left(\frac{\Delta x}{|\lambda_k^n|}\right), \tag{4.2}$$

between Δt and Δx in one spatial dimension where λ_k^n are the characteristic speeds, that is the eigenvalues of the flux Jacobian across the entire computational grid. The number c_{CFL} is the CFL factor and, generally, is given by

$$c_{CFL} \approx \frac{1}{2s-1},$$

where s is the formal order of the method [15].

The condition (4.2) allows us to treat the order of accuracy in terms of Δt to be the same as Δx.

4.2 The Modal Discontinuous Galerkin Method

Recall that there are three main classes of linear PDE: elliptic, parabolic, and hyperbolic. However, note that not all PDEs fit nicely into any of these. Generally, elliptic equations apply to static problems in elasticity, parabolic equations model time-dependent diffusion and heat, and hyperbolic equations describe wave propogation [6]. The hyperbolic nature of the Euler equations (both non-relativistic and relativistic) can give rise to discontinuities in the solution. As such, the more classical *(continuous) Galerkin methods* may give unsatisfactory results. The reader should consult works such as [6, 12, 14] for more information on these methods.

To describe the (modal) DG method, we consider a general conservation law

$$q_{,t} + \nabla \cdot \mathbf{F}(q) = 0, \quad \text{in } \Omega \subset \mathbb{R}^d, \tag{4.3}$$

where $q(t,x) : \mathbb{R}_{\geq 0} \times \mathbb{R}^d \to \mathbb{R}^m$ is a vector of conserved variables, the matrix $\mathbf{F}(q) : \mathbb{R}^m \to \mathbb{R}^{m \times d}$ is the flux function, d is the spatial dimension, and m is the number of equations in the system. Here, we denote by q the vector of conserved quantities for clarity. As a reference, equation (3.19) is of this form when $\mathbf{S} = 0$, which occurs in Minkowski spacetime using rectangular coordinates.

In order to appropriately dub (4.3) a conservation law, we state the following definitions.

Definition 4.1 *The flux Jacobians of* (4.3)*,* A^i*, are defined to be*

$$\mathbf{A}^i(q) := \frac{\partial \mathbf{F}^i}{\partial q},$$

where $i = 1, 2, 3$ *and* $\mathbf{F}^i$ *is the* i^{th} *column of the matrix* $\mathbf{F}$*. Alternatively, the vector* $\mathbf{F}^i$ *is the flux in the* i*-direction.*

The flux Jacobians play a pivotal role in the nature of the PDE. Namely, given the correct assumptions, we may have the following definition apply to the system (4.3).

Definition 4.2 *The PDE* (4.3) *is hyperbolic in* $q \in D \subset \mathbb{R}^m$ *if* $\mathbf{n} \cdot \mathbf{A}^i(q)$ *is diagonalizable with real eigenvalues* $\forall q \in D$ *and* $i = 1, 2, 3$ *with* $\|\mathbf{n}\| = 1$*.*

Suppose Ω is a polygonal domain with boundary $\partial\Omega$. Then we can find a *triangulation* $\mathcal{T}^h$, given a grid spacing h, such that we have $\Omega = \cup_{i=1}^{M} \mathcal{T}_i$ with $\mathcal{T}_i \in \mathcal{T}^h$. We call each $\mathcal{T}_i$ an element, and we require that no two elements overlap. In the one-dimensional case, the triangulation $\mathcal{T}^h$ is simply a mesh (usually uniform) while each element $\mathcal{T}_i$ is an interval of length h_i.

Consider the polynomial space $P^N(\mathbb{R}^d)$, that is the space of polynomials of degree at most N. Then we can define $[P^N]^m$ to be the vector space of column vectors with m components, each component belonging to a copy of $P^N(\mathbb{R})$.

This allows us to define the so-called broken finite element space [12, 14]

$$\mathcal{W}^h := \left\{ w^h \in [L^\infty(\Omega)]^m : w^h|_{\mathcal{T}_i} \in [P^N]^m, \forall \mathcal{T}_i \in \mathcal{T}^h \right\}. \tag{4.4}$$

Note that no continuity is assumed across the interfaces between different elements. This is, perhaps, the most obvious difference between the DG method and any given continuous Galerkin method. This is advantageous as we can approximate our discontinuous solution with a best approximation from this broken finite element space. Within each element $\mathcal{T}_i$, the approximate solution is thus a vector of polynomials, which means that we can express it in terms of the Legendre polynomials. That is, at time $t = t^n$, we have

$$q^h(t^n, x(\xi)) \Big|_{\mathcal{T}_i} = \sum_{\ell=1}^{L(d)} Q_i^{(\ell)n} \varphi^{(\ell)}(\xi). \tag{4.5}$$

where $\varphi^{(\ell)} \in P^N$ is the ℓ^{th} Legendre basis vector and $L(d)$ is the total number of Legendre basis vectors of at most degree d. The Legendre basis vectors are orthogonal in the sense that

$$\frac{1}{|\mathcal{T}_0|} \int_{\mathcal{T}_0} \varphi^{(k)}(\xi) \varphi^{(\ell)}(\xi)\, d\xi = \delta_{k\ell}, \tag{4.6}$$

where $\mathcal{T}_0$ is the reference element, $|\mathcal{T}_0|$ is its norm (length, area, or volume), and $\xi \in \mathcal{T}_0$ in $(4.3) - (4.5)$ are the reference coordinates. For instance, with one spatial dimension, we may choose $\mathcal{T}_0 = [-1, 1]$.

If we consider a first-order method, then we can see (in general, in fact) that the average value of the solution $q(t^n, x)$ in element $\mathcal{T}_i$ is the first Legendre coefficient in the expansion

(4.5). That is

$$\overline{q}(t^n, x(\xi))\Big|_{\mathcal{T}_i} = Q_i^{(1)n}. \tag{4.7}$$

We multiply the conservation law (4.3) by a Legendre test function $\varphi^{(k)}$ to exploit the expansion (4.5) and the orthogonality (4.6). On each element $\mathcal{T}_i$, we integrate by parts finding that

$$\frac{d}{dt}Q_i^{(k)} = \frac{1}{|\mathcal{T}_i|}\int_{\mathcal{T}_i} \nabla_{\mathbf{x}}\varphi^{(k)} \cdot \mathbf{F}\left(q^h|_{\mathcal{T}_i}\right)\, d\mathbf{x} - \frac{1}{|\mathcal{T}_i|}\oint_{\partial\mathcal{T}_i} \mathcal{F}\cdot\, ds \tag{4.8}$$

where $\nabla_{\mathbf{x}}\varphi^{(k)}$ is the gradient of $\varphi^{(k)}$ and $\mathcal{F}$ is the numerical flux [12]. In DoGPack, the numerical flux is found using the Rusanov solver, which we describe later in this chapter [15]. The ODE (4.8) can be found using integration-by-parts as suggest by [12, 14]. Now that we have an ODE, we can use an explicit Runge-Kutta (RK) method find the solution $Q_i^{(k)n}$ in each element $\mathcal{T}_i$. The reader is directed to [8] for an introduction or refresher on RK and other explicit time-stepping methods.

4.3 The Riemann Problem

Hyperbolic problems may exhibit discontinuities in the solution. As such, it is instructive to consider the following problem with initial data

$$\frac{\partial q}{\partial t} + \frac{\partial f}{\partial x} = 0, \qquad \text{such that} \qquad q(0,x) = \begin{cases} q_L & x < 0.5 \\ q_R & x > 0.5, \end{cases} \tag{4.9}$$

on $0 \le x \le 1$. This is known as the *Riemann problem*. The Riemann problem admits several kinds of weak solutions. Two of which are shocks and rarefactions [8, 14].

4.3.1 Shocks

In simplest terms, a shock is a propogating discontinuity in the variables $q(t,x)$. In one spatial dimension for the relativistic hydrodynamic equations, if the shock is located at x_s at

time t then $\mathbf{U}$ decomposes as

$$\mathbf{U} = \begin{cases} \mathbf{U}_L & x < x_s \\ \mathbf{U}_R & x > x_s, \end{cases} \tag{4.10}$$

where L and R are the initial states to the left and right of the discontinuity. If we take $\mathbf{U}_L$ and $\mathbf{U}_R$ to both be constant vectors, then equation (4.3) paired with these initial conditions are an instance of the Riemann problem. From the initial Riemann problem, the exact solution at some arbitrary time t can be surmised in some cases. For the special relativistic shock tube problem, there is indeed an exact solution. To find this solution, we may impose the *Rankine-Hugoniot jump conditions*

$$\mathbf{F}(\mathbf{U}_{L^*}) - \mathbf{F}(\mathbf{U}_{R^*}) = V_s(\mathbf{U}_{L^*} - \mathbf{U}_{R^*}), \tag{4.11}$$

where L^* and R^* represent the states to the left and right of the shock, which propogates at the speed V_s, at some arbitrary time. Since the shock travels, these two state are not constant.

In the special relativistic case, these jump conditions are

$$\begin{aligned} D_{L^*}v_{L^*} - D_{R^*}v_{R^*} &= V_s(D_{L^*} - D_{R^*}), \\ (S_{L^*}v_{L^*} + p_{L^*}) - (S_{R^*}v_{R^*} + p_{R^*}) &= V_s(S_{L^*} - S_{R^*}), \\ (S_{L^*} - D_{L^*}v_{L^*}) - (S_{R^*} - D_{R^*}v_{R^*}) &= V_s(\tau_{L^*} - \tau_{R^*}), \end{aligned} \tag{4.12}$$

which can be found in [10, 11]. In general, the Rankine-Hugoniot conditions connect the jump in the quantities q with the jump in the flux $f(q)$ through the speed of the propogating shock. The conditions come about when we impose the continuity of fluxes across the discontinuity. This still applies in the relativistic case between $\mathbf{U}$ and $\mathbf{F}(\mathbf{U})$.

It is important to stress that the subscripts L^* and R^* represent the states to the left and right of the propogating shock, not of the initial shock location x_s. In the interval $0 \leq x \leq 1$, the initial shock location is usually taken to be $x_s = 0.5$. In this case $\mathbf{U}(t = 0, x < 0.5) = \mathbf{U}_L$ and $\mathbf{U}(t = 0, x > 0.5) = \mathbf{U}_R$. However, after some time t, the shock will propogate with speed V_s so that, for example, $\mathbf{U}(t, x - 0.5 < tV_s) = \mathbf{U}_{L^*}$.

This is important to keep in mind when a problem contains multiple shocks and other kinds of structures where we may have left, right, and middle states [8].

4.3.2 Rarefactions

Shocks are not the only possible structures present when we have discontinuous initial data. Whereas a shock takes on a flow profile discontinuous at a point, a *rarefaction* is a smooth profile where fluid, as one might expect, rarefies (as opposed to compressing). In order to characterize a rarefaction, we look for a so-called self-similar solution to the conservation law (4.3), i.e. when we have that $q(t,x) = \tilde{q}((x-x_0)/t)$, where x_0 divides the initial left and right states.

For more information on rarefaction waves, see [10, 11].

4.3.3 An Approximate Riemann Solver: The Rusanov Solver

While we may be able to find a few weak solutions to the Riemann problem, the general solution may not have an analytical form. This brings us to the idea of an *approximate Riemann solver* [8, 14]. In the DG implementation, the numerical solution may be piecewise constant. As an effect, each cell interface (where elements $\mathcal{T}_i$ and $\mathcal{T}_{i+1}$ meet) we have a Riemann problem with initial data given by the constant values $Q_i^{(0)n}$ and $Q_{i+1}^{(0)n}$.

We use the *Rusanov approximate Riemann solver* in DoGPack [17, 15]. Another name for the Rusanov solver is the *local Lax-Friedrichs flux* ([14], p 438). The numerical flux $\mathcal{F}$ is a result of the boundary term in the integral on the right-hand side of (4.8). It is an approximation of the flux $\mathbf{F}(\mathbf{U})$ through the boundaries of the current cell using neighboring cells [9]. The numerical flux is chosen to be

$$\mathcal{F}(\mathbf{U}_L, \mathbf{U}_R) = \frac{1}{2}(\mathbf{F}(\mathbf{U}_L) + \mathbf{F}(\mathbf{U}_R)) - \frac{\lambda}{2}(\mathbf{U}_R - \mathbf{U}_L), \tag{4.13}$$

where

$$\lambda = \max(|\lambda_R|, |\lambda_L|), \tag{4.14}$$

and

$$\begin{aligned} \lambda_L &= \min(\lambda_-(\mathbf{U}_L), \lambda_-(\bar{\mathbf{U}})), \\ \lambda_R &= \max(\lambda_+(\mathbf{U}_R), \lambda_+(\bar{\mathbf{U}})), \end{aligned} \tag{4.15}$$

are the left- and right-going wave speeds determined by $\lambda_\pm$ which are described in Chapter 5 for each test case and $\bar{\mathbf{U}}$ is the so-called *Roe average*. In DoGPack, we simply take the Roe average to be the arithmetic average, i.e. $\bar{\mathbf{U}} = (\mathbf{U}_L + \mathbf{U}_R)/2$ [15]. For a full review on Roe averages, see for example [8].

We note that the Rusanov flux $\mathcal{F}$ is *consistent* in the sense that

$$\mathcal{F}(\mathbf{U}, \mathbf{U}) = \mathbf{F}(\mathbf{U}),$$

which is essential for a numerical flux [8].

4.4 Shock Capturing Limiters

When applying a high-order method to a hyperbolic problem, the numerical solution exhibits smoothing or even oscillations near shocks [9, 14]. The following is often referred to as *Godunov's theorem*; it applies to numerical schemes for solving PDEs.

Theorem 4.3 *A linear, constant-coefficient and monotonicity-preserving (i.e. one that generates no new local extrema) scheme is at most first-order accurate.*

We see that there are limitations to any scheme for PDEs which is linear. If we want a linear (in the sense that the solution at $t = t^{n+1}$ depends on the previous time linearly) scheme that does not create these artificial oscillations, then we are forced to accept first-order accuracy. Otherwise, we must employ nonlinear methods for solving the PDE.

A *shock-capturing limiter* is a means of achieving high order in a numerical scheme in such as way as to work around Godunov's theorem. While limiters are applied to various numerical approaches including classical finite volume methods to weighted non-oscillatory (WENO) schemes, we focus on limiters built for DG methods. The basic idea of a limiter is to "dampen" the oscillations. We give a more precise sense of this in the next two subsections.

4.4.1 The Moment Limiter

Consider the function

$$\text{minmod}(a,b,c) = \begin{cases} \text{sgn}(a)\min(|a|,|b|,|c|) & \text{if } \text{sgn}(a) = \text{sgn}(b) = \text{sgn}(c) \\ 0 & \text{otherwise .} \end{cases} \tag{4.16}$$

The limiter we employ in our DoGPack simulations is the *moment limiter*, which is a generalization of the minmod limiter [9, 15]. The choice of a, b, and c are key as we shall see.

For a scalar conservation law, recall that we express the approximate solution in terms of the Legendre basis on the reference element, which is given by (4.5). In the limiter proposed by Krivodonova, we limit the numerical solution by

$$\tilde{Q}_i^{(\ell)n} = \text{minmod}\left(Q_i^{(\ell)n}, \alpha_\ell(Q_{i+1}^{(\ell-1)n} - Q_i^{(\ell-1)n}), \alpha_\ell(Q_i^{(\ell-1)n} - Q_{i-1}^{(\ell-1)n})\right), \tag{4.17}$$

where we can have $\frac{1}{2}(2\ell-1)^{-1} \leq \alpha_\ell \leq 1$ but $\alpha_\ell = 1$ is the proposed choice [7]. The limiting is performed from the highest order Legendre coefficient down to the first. That is, we start at $\ell = L(d)$ and replace $\tilde{Q}_i^{(\ell)n} \leftarrow Q_i^{(\ell)n}$. If we have that $\tilde{Q}_i^{(\ell)n} = Q_i^{(\ell)n}$ or $\ell = 1$ we stop. Otherwise, we move on to limiting the $\ell - 1$ coefficient and so on.

It turns out that since the relativistic hydrodynamic equations form a nonlinear system rather than a scalar law, we must apply the moment limiter not to the conserved variables $\mathbf{U}$, but the characteristic variables $\mathbf{LU}$, where $\mathbf{L}$ is the matrix of left eigenvectors of the flux Jacobian $\mathbf{A}^i$ [7]. As given by Krivodonova, we would have

$$(\mathbf{L}\tilde{\mathbf{U}}_i^{(\ell)})_j = \text{minmod}\left((\mathbf{L}\mathbf{U}_i^{(\ell)})_j, (\mathbf{L}(\mathbf{U}_{i+1}^{(\ell-1)} - \mathbf{U}_i^{(\ell-1)}))_j, (\mathbf{L}(\mathbf{U}_i^{(\ell-1)} - \mathbf{U}_{i-1}^{(\ell-1)}))_j\right), \tag{4.18}$$

where $(\mathbf{L}\tilde{\mathbf{U}}_i^{(\ell)})_j$ is the ℓ^{th} Legendre coefficient of the j^{th} characteristic variable in element i.

4.4.2 A New High-Order Shock Capturing Limiter

Recently, a shock-capturing limiter based on the Barth-Jespersen limiter which is simple to implement has been developed [2, 12].

For a scalar problem, i.e. when $m = 1$, the procedure is as follows, adopted directly from [12]:

Step 0. Let χ_i be a set of points in element $\mathcal{T}_i$ used to compute cell extrema. The DoGPack implementation uses Gaussian quadrature nodes and edge Gaussian quadrature points.

Step 1. In each element $\mathcal{T}_i$, compute the approximate extrema:

$$q_{M_i} := \max_{x \in \chi_i} \left(q^h(x) | \mathcal{T}_i \right) \quad \text{and} \quad q_{m_i} := \min_{x \in \chi_i} \left(q^h(x) | \mathcal{T}_i \right).$$

Step 2. Denote the neighbors of $\mathcal{T}_i$ by $N_{\mathcal{T}_i}$, excluding $\mathcal{T}_i$ itself. We use these for the upper bound

$$M_i := \max \left(\overline{q}_i + \alpha(h), \max_{j \in N_{\mathcal{T}_i}} (q_{M_j}) \right) \tag{4.19}$$

and the lower bound

$$m_i := \max \left(\overline{q}_i - \alpha(h), \min_{j \in N_{\mathcal{T}_i}} (q_{m_j}) \right). \tag{4.20}$$

The scalar function $\alpha(h) \geq 0$ is essential and is called the *tolerance function.*

Step 3. Let

$$\theta_{M_i} := \phi \left(\frac{m_i - \overline{q}_i}{q_{M_i} - \overline{q}_i} \right) \quad \text{and} \quad \theta_{m_i} := \phi \left(\frac{M_i - \overline{q}_i}{q_{m_i} - \overline{q}_i} \right)$$

with $0 \leq \phi(y) \leq 1$ is a cutoff function which limits the higher order terms in the expansion (3.4).

Step 4. The *rescaling parameter* is defined as

$$\theta_i := \min(1, \theta_{m_i}, \theta_{M_i}). \tag{4.21}$$

Step 5. The approximate solution is rescaled according to the rescaling parameter so that

$$\tilde{q}^h(x)|_{\mathcal{T}_i} := \overline{q}_i + \theta_i \left(q^h(x)|_{\mathcal{T}_i} - \overline{q}_i \right). \tag{4.22}$$

It can be shown that, if we require $\alpha(h) = \mathcal{O}(h^r)$ for $r < 2$ then we have

$$|q(x) - q(\xi_0)| = \mathcal{O}(h^2) \leq \alpha(h) \quad \text{for all} \quad |x - \xi_0| = \mathcal{O}(h) \tag{4.23}$$

Notice that setting $\alpha(h) = 0$ is equivalent to not using a limiter at all. This ensures that $\alpha(h)$ does not vanish too rapidly and that true local extrema are not clipped. On the other hand, nonvanishing $\alpha(h)$ allows for nonphysical oscillations. A few test cases ranging from a 1D periodic advection problem, to 2D Riemann problems are studied in [12].

The extension to a system of equations is simple, and can be used on either primitive or conserved variables. Of course, we would choose the conserved variables $\mathbf{U} := (D, S_1, S_2, S_3, \tau)$ for our relativistic test cases. Because it is simply an extension to the above, we omit the procedure but direct the reader to [12]. We do mention that the limiter chooses the same rescaling parameter for all variables.

4.4.3 The Admissible Set of States

Because of the oscillations inherent in higher order schemes, we may be presented with physically impossible numerical solutions. For example, the pressure of the gas may oscillates so that in some regions we have $p < 0$, which we do not allow for in perfect fluids or dust. We may also have a situation where the speed of the fluid near the shock oscillates to a value above the speed of light. We thus need to prescribe a maximum (or positivity) principle to these variables.

In terms of the primitive variables we thus have an admissible set $\mathcal{G}$ such that

$$\mathcal{G} := \left\{ \mathbf{U} = (D, S_j, \tau)^T | \rho(\mathbf{U}) > 0, p(\mathbf{U}) > 0, v(\mathbf{U}) < 1 \right\} \tag{4.24}$$

where we define $v := \sqrt{v^i v_i} = \sqrt{\gamma_{ij} v^i v^j}$.

In the DoGPack code we use the conserved variables so that we may cast the hydrodynamic equations as a balance law. While we do have the capability to convert between the two sets of variables through the use of a root-finding algorithm, we would much prefer to cast $\mathcal{G}$ solely in terms of $\mathbf{U} = (D, S_j, \tau)$ rather than $\mathbf{V}$. This will cut down on CPU time.

Consider the set $\mathcal{G}_1$ defined as

$$\mathcal{G}_1 := \left\{ \mathbf{U} = (D, S_j, \tau)^T | D > 0, g(\mathbf{U}) := \tau + D - \sqrt{D^2 + S^2} > 0 \right\}. \tag{4.25}$$

It can be proven that $\mathcal{G}_1$ is equivalent to $\mathcal{G}$, and that $\mathcal{G}_1$ is a convex set [20].

We note that the admissible state given by (3.24) can be enforced even using the moment limiter, as the option is available in DogPack. Indeed, the pressure is notorious in possibly causing issues if postivity is not enforced [7].

4.5 Recovery of the Primitive Variables

Although the transformation from primitive variables $\mathbf{V}$ to conserved variables $\mathbf{U}$ is straightforward, the recovery is not. That is, we cannot simply invert the relationship between the conserved and primitive variables. For Minkowski spacetime, we follow the work of Del Zanna et al defining the quantity $H := \rho h W$ so that the conserved variabes can be written as

$$\mathbf{U} = (D, S_j, \tau) = (\rho W, H v_j, H - p - D)^T. \tag{4.26}$$

We need to invert this system to find $\mathbf{V}(\mathbf{U})$. To do so, note that

$$\begin{aligned} S^j S_j &= H^2 v^j v_j \\ &= H^2 (1 - W^{-2}) \end{aligned} \tag{4.27}$$

from the definition of the Lorentz factor.

If we can determine W, then the primitive variables will follow. Thus, we seek to find the root of the function

$$f(W) := H(W)^2 (1 - W^{-2}) - S^j S_j \tag{4.28}$$

which will give us the desired Lorentz factor. From the Lorentz factor W we can recover the primitive variables by noting that $\rho = D/W, v_j = S_j/H = S_j/(\rho h W)$ and $p = H - (\tau + D) = \rho h W - \tau - D$. The quantity H can be written solely in terms of the conserved variables as

$$H(W) = \frac{E\Gamma_1 W^2 - DW}{\Gamma_1 W^2 - 1} \tag{4.29}$$

which is needed in order to implement the root-finding technique of choice [4].

In the DoGPack code, we use the Newton-Raphson method to find this root, with the initial guess determined by employing the bisection method. The initial interval can be taken as $W \in [1, 70]$ which correspond to speeds $v \in [0, 0.99]$ in the special relativistic case [15].

In the $3 + 1$ splitting of spacetime, the above recovery is readily applicable since

$$\mathbf{U} = (D, S_j, \tau) = (\rho W, H v_j, H - p - D)^T \tag{4.30}$$

but with the key difference of $W = \alpha u^t$. However, $\alpha u^t = (1 - v_i v^i)^{-1/2}$ so that only the quadrature rule to find the quantity $v_i v^i$ differs.

CHAPTER 5. TESTS AND RESULTS

5.1 The Special Relativistic Shock Tube

The simplest numerical simulation of a hyperbolic system containing discontinuities is the so-called shock tube, which is a one-dimensional test. In a simple shock tube problem, the initial data is a Riemann problem. The shock location, which is where the discontinuity is located, is usually in the center of the interval. In which case, we dub the two states $\mathbf{U}_L$ and $\mathbf{U}_R$.

In Minkowski spacetime, the $3+1$ foliation of spacetime is trivial with $\alpha = 1$ and $\beta^i = 0$. The conserved variables and fluxes are simply

$$\mathbf{U} = \left(\rho W, \rho h W^2 v^j, \rho h W^2 - p - \rho W\right)^T, \tag{5.1}$$

$$\mathbf{F}^i = \left(\rho W v^i, \rho h W^2 v^i v^j + p\delta^{ij}, \rho h W^2 v^i - \rho W v^i\right)^T, \tag{5.2}$$

where $W = (1 - v_i v^i)^{-1/2} = \alpha u^t$ is the simple Lorentz boost. In fact, for each i we have v^i being equal to v_i and $v^0 = 0 = v_0$. As stated earlier, there is no source term, leading to the conservation law

$$\partial_t \mathbf{U} + \partial_i \mathbf{F}^i = 0. \tag{5.3}$$

5.1.1 The Blast Wave

In one spatial dimension, the eigenvalues of the flux Jacobian $\mathbf{A}^x$ are simple being

$$\begin{aligned} \lambda_0 &= v^x, \\ \lambda_\pm &= \frac{v^x \pm c_s}{1 \pm v^x c_s}, \end{aligned} \tag{5.4}$$

where

$$c_s^2 = a^2 \left(1 + \frac{a^2}{\Gamma - 1}\right)^{-1} = \frac{\Gamma p}{\rho h}, \tag{5.5}$$

is the relativistic sound speed within the perfect fluid [11], and a is the classical, non-relativistic sound speed. These characterstic speeds differ from the Newtonian limit ($v^x << c$) but do reduce to their non-relativistic Euler counterparts. The speed λ_0 has multiplicity 3 [4]. For the corresponding eigenvectors, the reader may consult [11, 14]. The two maximal speeds $\lambda_\pm$ are those that are used in the Rusanov solver.

We enact two separate initial conditions, which are studied in various works [11, 4].

$$\text{Blast wave:} \quad \begin{cases} (\rho_L, v_L, p_L) &= (10, 0, 13.3) \\ (\rho_R, v_R, p_R) &= (1, 0, 10^{-6}). \end{cases} \tag{5.6}$$

When no limiter is applied, we see in **Figs 5.1-5.3** oscillations in the presence of the shock as well as both ends of the rarefaction. These oscillations are nonphysical and must be dampened. The moment limiter described in the previous chapter and in [7] is then applied, with plots shown on the right for the density ρ, velocity v^x, and the pressure p. The exact solutions were plotted in Python using the exact Riemann solver provided in [10, 11]. We do note, however, that the numerical solution fits well with the exact solution in smooth regions whether or not the limiter is applied. This is expected since the higher order Legendre coefficients in the expansion (4.5) become smoother functions as $\ell \to L(d)$.

5.2 Accretion onto a Black Hole

To show the viability of implementing astrophysical simulations in DoGPack, we discuss and present accretion onto a black hole. The cases of dust and a perfect fluid are well-understood

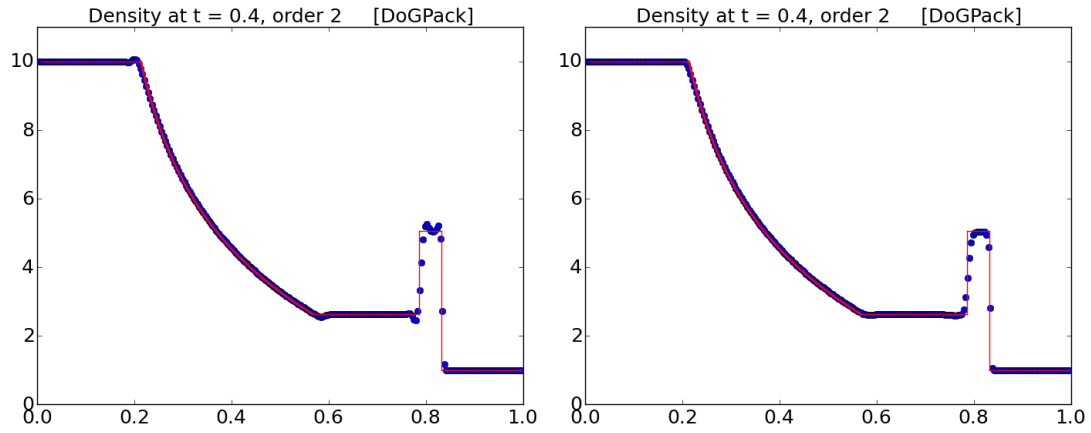

FIGURE 5.1: The density ρ computed using DoGPack in blue and the exact solution red at time $t = 0.4$ for the blast wave. On the left no limiter is applied. On the right the moment limiter is used.

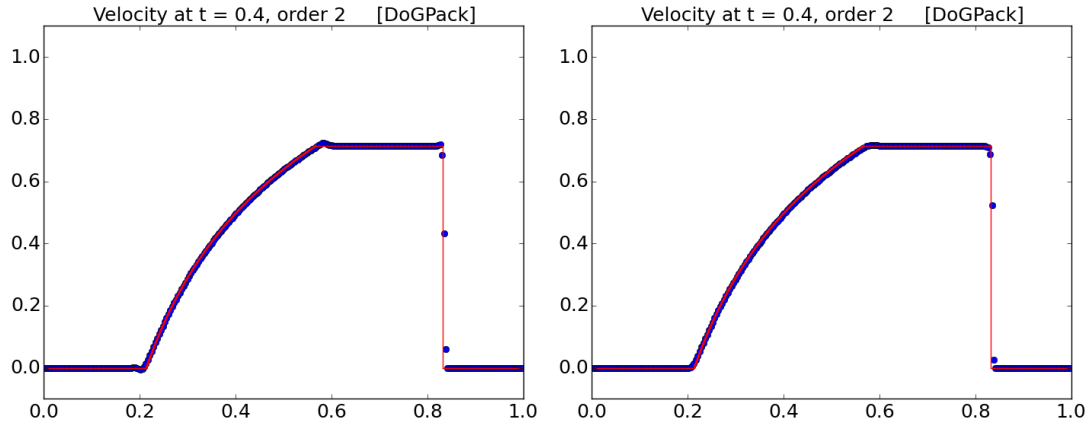

FIGURE 5.2: The speed v^x computed using DoGPack in blue and the exact solution red at time $t = 0.4$ for the blast wave. On the left no limiter is applied. On the right the moment limiter is used.

in the Schwarzschild spacetime and can be found in works such as [1, 13]. Accretion onto a black hole is an example of smooth flow.

By dust accretion, we mean a fluid such that $p \approx 0$. The simulation considers a one-dimensional slice of the Schwarzschild spacetime. In this scenario, we only need information from the flux Jacobian $\mathbf{A}^r$. The eigenvalues for the Rusanov solver are

$$\begin{aligned} \lambda_0 &= \alpha v^r - \beta^r, \\ \lambda_\pm &= \frac{\alpha}{1 - v^2 c_s^2} \left[v^r (1 - c_s^2) \pm c_s \sqrt{(1 - v^2)[\gamma^{rr}(1 - v^2 c_s^2) - v^r v^r (1 - c_s^2)]} \right] - \beta^r. \end{aligned} \tag{5.7}$$

Note that λ_0 has multiplicity 3 [14]. The corresponding eigenvectors can be written in terms of the metric and primitive variables, but for the sake of brevity we do not include them in this thesis. The reader is directed to [14] for the eigenvectors in explicit form.

5.2.1 Steady-State Solution

For dust, the steady-state solution is known and indeed simple in Eddington-Finkelstein coordinates. The exact solution for the density and radial velocity are given by

$$\rho_\infty(r) = \frac{0.195}{\sqrt{2Mr^3}}, \tag{5.8}$$

and

$$v^r_\infty(r) = -\frac{1}{\sqrt{1 + r/2M} \left(1 + \sqrt{2M/r} + 2M/r \right)}, \tag{5.9}$$

on $0 < r < \infty$ [13]. The expression for the velocity is that of v^r in the $3 + 1$ splitting, while other formulations of the relativistic Euler equations result in different expressions of the velocity [16]. The fact that the radial velocity is negative reassures us that the dust flows into the black hole, and since there is no singularity at $r = 2M$, it will pass through the event horizon unhinged.

In **Fig. 5.4** we see that the simulation behaves well in the computational domain $0.5M \leq r \leq 15M$, with the choice $M = 1$. For $r \leq 2M$, the fluid is at or within the event horizon but the flow is still smooth. This is consistent with the exact solution in that the only singularity

occurs at $r = 0$. As stated above, the event horizon $r = 2M$ does not affect the density nor velocity. However, given the nature of $r = 0$, we delete the region $r < 0.5M$ in the simulation.

It should be noted that in the case of a perfect fluid where the pressure is not negligible, we cannot express the velocity in closed form as in (5.9). However, we may numerically solve an ODE as is done by Papadopoulos and Font [13]

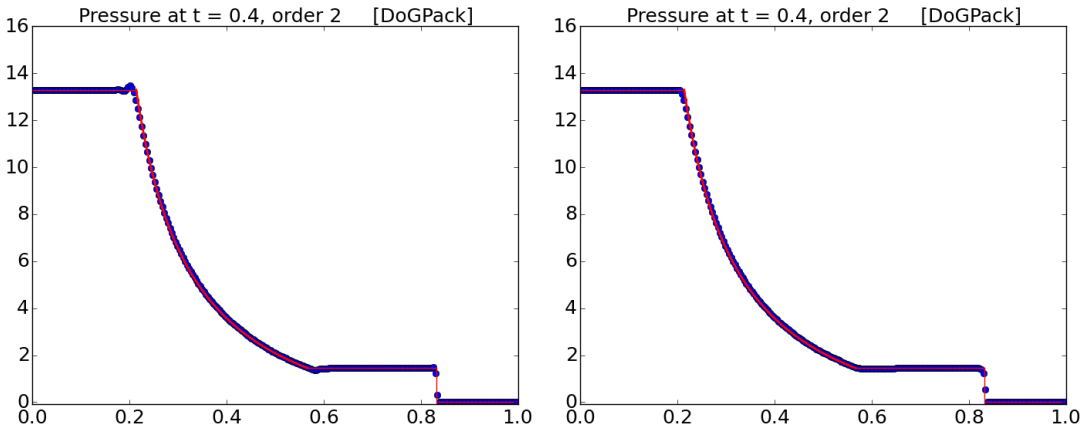

FIGURE 5.3: The pressure p computed using DoGPack in blue and the exact solution red at time $t = 0.4$ for the blast wave. On the left no limiter is applied. On the right the moment limiter is used.

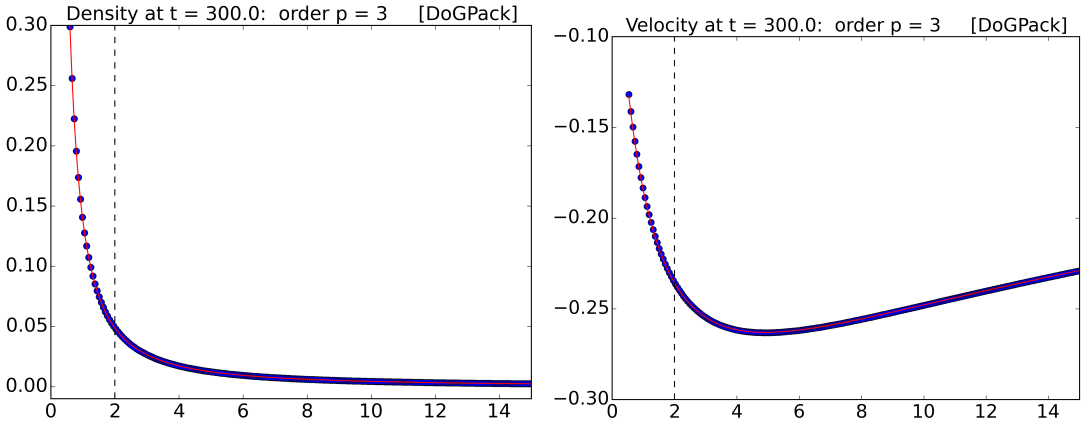

FIGURE 5.4: The variables ρ (left) and v^r (right) computed using DoGPack in blue and the exact solution red at time $t = 0.4$ for dust accretion into a black hole. The dashed lines represent the Schwarzschild radius, $r = 2M$.

CHAPTER 6. FUTURE WORK

The background and findings in this thesis serve as the groundwork for increasing DoGPack's versatility in the relativistic regime. We describe below several improvements and enhancements to the relativistic DoGPack libraries use for this thesis.

6.1 The Paralellization of DoGPack

To prepare for numerical simulations that would require more memory, we seek to parallelize DoGPack using the Message Passing Interface (MPI) and OpenMP. We remind the reader that MPI allows the user to distribute work across multiple processors via message-passing. MPI can be implemented in Fortran, C, C++, and Java.

One possible means of paralellization is to divide the computational domain among the processors as evenly as possible. In this way, the implementation is straightforward, but will help in load-balancing.

6.2 Magnetohydrodynamics and Relativity

Given that this thesis focuses on astrophysical simulations, we naturally seek to include problems involving plasmas. In order to properly describe a plasma, we require an understanding of electromagnetism in the context of relativity.

For a plasma in Minkowski spacetime, we have the *relativistic magnetohydrodynamics equations*

$$\partial_\alpha(\rho u^\alpha) = 0 \tag{6.1}$$

$$\partial_\alpha[(w+|b|^2)u^\alpha u^\beta - b^\alpha b^\beta + (p+|b|^2/2)g^{\alpha\beta}] = 0 \tag{6.2}$$

$$\partial_\alpha(u^\alpha b^\beta - u^\beta b^\alpha) = 0 \tag{6.3}$$

where b^β is the so-called magnetic induction four-vector [**?**]. One key difference in (6.1) – (6.3) from the SRHD equations is the inclusion of the magnetic induction equation. As pointed out by Del Zann et al, the induction equation is of Hamilton-Jacobi kind, and is not a hyperbolic conservation law.

6.3 GRHD in Multiple Spatial Dimensions

The tests presented in this thesis were one-dimensional in nature. However, the hydrodynamic equations (3.19) are inherently multidimensional as the metric of a black hole, for instance, describes the spacetime around a three-dimensional object. Although many flows involving a black hole may be regarded as one-dimensional, e.g. spherical accretion, there are many simulations which require more than one dimension.

One complication with even two-dimensional flows is the presence of the Lorentz factor which couples v^x and v^y. As pointed out by LeVeque, the Newtonian Euler equations exhibit transverse velocities which are constant across shocks. More significantly, we would have to solve a system of coupled ODEs across rarefaction waves solely for the transverse velocities [9].

6.4 Solving the Einstein Equations

In this thesis and in the extensions outlined above, the metric of spacetime is assumed to be stationary. This is a valid approximation assuming the mass-energy of the fluid is negligible compared to that of the black hole [14]. In general, the metric may not be known so we must put to use the *Einstein equations*

$$G_{\mu\nu} + \Lambda g_{\mu\nu} = 8\pi T_{\mu\nu} \tag{6.4}$$

where Λ is the cosmological constant, $G_{\mu\nu}$ is the *Einstein tensor* given by

$$G_{\mu\nu} := R_{\mu\nu} - \frac{1}{2} R g_{\mu\nu}, \tag{6.5}$$

and $R_{\mu\nu}$ is the *Ricci tensor* with *Ricci scalar* $R := g^{\mu\nu} R_{\mu\nu}$ [14]. The Ricci tensor is a symmetric rank 2 tensor which is a function of the Christoffel symbols and their derivatives. For an explicit expression of the Ricci tensor, see for example [14, 18, 3].

Rezzolla and Zanotti point out that the 3+1 splitting and its variations exploit spacetime in a way convenient for numerical simulations involving both the hydrodynamic equations and Einstein's equations. These simulations may vary from spherical collapse of stars to even gravitational waves propogating in spacetime.

BIBLIOGRAPHY

[1] Banyuls, F., Font, J. A., Ibanez, J. M., Marti, J. M., and Miralles, J. (1997). Numerical 3+1 General Relativistic Hydrodynamics: A Local Characteristic Approach. *The Astrophysical Journal*, (476):221–231.

[2] Barth, T. J. and Jespersen, D. C. (1989). The design and application of upwind schemes on unstructured meshes. *AIAA-89-0366*.

[3] Carroll, S. M. (1997). Lecture Notes on General Relativity.

[4] Del Zanna, L. and Bucciantini, N. (2002). An efficient shock-capturing central-type scheme for multidimensional relativistic flows: I. Hydrodynamics. *arXiv*.

[5] Gourgoulhon, E. (2007). 3+1 Formalism and Bases of Numerical Relativity.

[6] Johnson, C. (1987). Dover Publications, Inc.

[7] Krivodonova, L. (2007). Limiters for high-order discontinuous Galerkin methods. *Journal of Computational Physics*, (226):879–896.

[8] LeVeque, R. J. (2004). Cambridge University Press.

[9] LeVeque, R. J., Mihala, D., Dorfi, E., and Muller, E. (1997). Computational Methods for Astrophysical Fluid Flow.

[10] Lora-Clavijo, F., Cruz-Perez, J., Guzman, S., and Gonzalez, J. (2013). Exact solution of the 1D riemann problem in Newtonian and relativistic hydrodynamics. *Revista Mexicana de Fisica*, E(59):28–50.

[11] Marti, J. M. (2003). Numerical Hydrodynamics in Special Relativity. *Living Rev. Relativity*, 6(7).

[12] Moe, S. A., Rossmanith, J. A., and Seal, D. C. (2015). A Simple and Effective High-Order Shock-Capturing Limiter for Discontinuous Galerkin Methods. *arXiv*.

[13] Papadopoulos, P. and Font, J. A. (1998). Relativistic Hydrodynamics around Black Holes and Horizon Adapted Coordinate Systems. *arXiv*.

[14] Rezzolla, L. and Zanottia, O. (2013). Oxford University Press, first edition.

[15] Rossmanith, J. et al. (2016). DogPack [computer software].

[16] Rossmanith, J. A. (2006). High-Order Residual Distribution Schemes for Steady 1D Relativistic Hydrodynamics. *Hyperbolic Problems: Theory, Numerics, and Applications II*, pages 259–266.

[17] Rusanov, V. V. (1961). Calculation of Intersection of Non-Steady ShockWaves with Obstacles. *J. Comput. Math. Phys. USSR*, (1):267–279.

[18] Schutz, B. (2009). Cambridge University Press, second edition.

[19] Schwarzschild, K. (1916). Uber das Gravitationsfeld eines Massenpunktes nach der Einstein'schen Theorie.

[20] Wu, K. and Tang, H. (2015). High-order accurate physical-contraints-preserving finite difference WENO schemes for special relativistic hydrodynamics. *arXiv*.